Neuro-Oncology

Neuro-Oncology 16(4), 594–602, 2014
doi:10.1093/neuonc/not225
Advance Access date 9 December 2013

Hippocampal sparing radiotherapy for pediatric medulloblastoma: impact of treatment margins and treatment technique

N. Patrik Brodin, Per Munck af Rosenschöld, Malin Blomstrand, Anne Kiil-Berthlesen, Christian Hollensen, Ivan R. Vogelius, Birgitta Lannering, Søren M. Bentzen, and Thomas Björk-Eriksson

Department of Oncology, Sahlgrenska University Hospital, Gothenburg, Sweden (M.B.); Centre for Brain Repair and Rehabilitation, Institute of Neuroscience and Physiology, University of Gothenburg, Gothenburg, Sweden (M.B.); Radiation Medicine Research Center, Department of Radiation Oncology, Rigshospitalet, Copenhagen, Denmark (N.P.B., P.M.R., A.K.-B., C.H., I.R.V., S.M.B.); Niels Bohr Institute, University of Copenhagen, Copenhagen, Denmark (N.P.B., P.M.R.); Department of Clinical Physiology and Nuclear Medicine, Centre of Diagnostic Investigations, Copenhagen, Denmark (A.K.-B.); Department of Pediatric Oncology, the Queen Silvia Children's Hospital, University of Gothenburg, Gothenburg, Sweden (B.L.); Department of Human Oncology, University of Wisconsin Medical School, Madison, Wisconsin (S.M.B.); Department of Radiation Oncology, Sahlgrenska University Hospital, Gothenburg, Sweden (T.B.-E.)

Corresponding author: N. Patrik Brodin, PhD, Department of Radiation Oncology, Rigshospitalet, Blegdamsvej 9, DK-2100, Copenhagen, Denmark (brodin.patrik@gmail.com).

Background. We investigated how varying the treatment margin and applying hippocampal sparing and proton therapy impact the risk of neurocognitive impairment in pediatric medulloblastoma patients compared with current standard 3D conformal radiotherapy.

Methods. We included 17 pediatric medulloblastoma patients to represent the variability in tumor location relative to the hippocampal region. Treatment plans were generated using 3D conformal radiotherapy, hippocampal sparing intensity-modulated radiotherapy, and spot-scanned proton therapy, using 3 different treatment margins for the conformal tumor boost. Neurocognitive impairment risk was estimated based on dose-response models from pediatric CNS malignancy survivors and compared among different margins and treatment techniques.

Results. Mean hippocampal dose and corresponding risk of cognitive impairment were decreased with decreasing treatment margins ($P < .05$). The largest risk reduction, however, was seen when applying hippocampal sparing proton therapy—the estimated risk of impaired task efficiency (95% confidence interval) was 92% (66%–98%), 81% (51%–95%), and 50% (30%–70%) for 3D conformal radiotherapy, intensity-modulated radiotherapy, and proton therapy, respectively, for the smallest boost margin and 98% (78%–100%), 90% (60%–98%), and 70% (39%–90%) if boosting the whole posterior fossa. Also, the distance between the closest point of the planning target volume and the center of the hippocampus can be used to predict mean hippocampal dose for a given treatment technique.

Conclusions. We estimate a considerable clinical benefit of hippocampal sparing radiotherapy. In choosing treatment margins, the trade-off between margin size and risk of neurocognitive impairment quantified here should be considered.

Keywords: medulloblastoma, hippocampal sparing, tumor bed boost, cognitive risk estimation.

Medulloblastoma (MB) is the most common malignant brain tumor in children, accounting for ~20% of all pediatric CNS malignancies.[1] Radiotherapy plays a vital role in the treatment of MB and given together with surgery and post-irradiation chemotherapy results in 5-year survival rates of 75%–85% for standard-risk patients (without CNS metastases, CSF involvement, large unresected tumor, or biological high-risk factors).[2] Age is also an important factor in MB risk stratification, and very young children (<3 y) are treated according to different regimens than older children. Although effective, this aggressive treatment is associated with a considerable risk of late side effects, of which neurocognitive decline is one of the most devastating and, unfortunately, most common.[1,3] Irradiation of the CNS is a major contributor to this decline, and a relationship between radiation dose to the brain and cognitive impairment has been reported in several studies of pediatric brain tumor patients.[4–9]

Specifically, a strong correlation has been shown between cognitive outcome[4,8,10] and dose to the hippocampus (referring to

Received 22 May 2013; accepted 30 October 2013

both the left and the right hippocampus as one common structure) and the temporal lobe. The hippocampus, one of the major sites of neurogenesis in the adult brain of humans[11] and rodents,[12] is situated within the temporal lobe. Neurogenesis is thought to be important for memory formation,[13,14] and cognitive deficits have been reported after radiation-induced impaired hippocampal neurogenesis in rodents.[15,16] Hence, the hippocampus is arguably the main risk organ for cognitive deficits after brain irradiation. Accordingly, reducing the hippocampal radiation dose would likely reduce the risk of late neurocognitive side effects. We hypothesize that this can be achieved using modern inverse-planned radiotherapy techniques with dose-volume constraints set to limit the dose to the hippocampus while still treating the planning target volume (PTV) to a high dose. We previously demonstrated the feasibility of sparing the hippocampus and subventricular zone (SVZ) in whole-brain irradiation of MB, with little anatomical variation among patients.[17] When considering the high-dose boost, however, the variation among individuals is considerably larger.

The radiotherapy target volume in MB has remained fairly constant with whole craniospinal irradiation (CSI) of 23.4–36 Gy and a high-dose boost to the posterior fossa (PF) to 54–55.8 Gy. Many centers are now moving away from whole PF irradiation in favor of boosting only the primary tumor bed including a safety margin.[6,18–22] This introduces some heterogeneity among patients in the target for the high-dose boost, dependent on the extent and anatomical position of the primary tumor. The efficacy of a conformal tumor bed boost compared with treating the whole PF is being tested in the ongoing randomized ACNS0331 trial. Despite promising results reported from prospective cohort studies of a conformal tumor bed boost, there is still no consensus regarding what margin should be added to the tumor bed (gross tumor volume [GTV]) to yield the clinical target volume (CTV).[6,18–22] The GTV to CTV margins applied in published reports range from 0.5 to 1.5 cm, all with a further 0.5-cm margin to yield the corresponding PTV.

In this study, we analyzed how the size and position of the primary tumor bed as well as application of different treatment margins to the tumor bed would influence the dose to the hippocampus and whether a hippocampal sparing approach for the boost treatment would be predicted to yield a clinically relevant reduction in dose. We estimated the risk of cognitive decline using published dose-response models for late neurocognitive impairment based on long-term follow-up of CNS patients in the childhood cancer survivor study.[4] We compared conventional 3-dimensional conformal radiotherapy (3D CRT) with 2 hippocampal sparing techniques: intensity-modulated radiotherapy (IMRT) and spot-scanned proton therapy (PT).

Materials and Methods

Patient Material and Treatment Planning

Seventeen pediatric MB patients were included in this study, of whom 13 were treated at Rigshospitalet in Copenhagen, Denmark in 2004–2009 and 4 were treated at Sahlgrenska University Hospital in Gothenburg, Sweden in 2002–2007. The median age at treatment was 6 years (range, 4–15 y). A criterion for inclusion was retrievable preradiotherapy CT and MRI scans. Different definitions of GTV are used for MB patients in various studies; in this analysis GTV was defined as the postoperative tumor bed including the operation cavity. Figure 1 illustrates the difference between this definition and defining the GTV as the preoperative tumor bed, for a patient in whom this difference was apparent. The GTV, PF, and hippocampus were delineated on fused transversal CT and T1-weighted MRI scans by an experienced neuroradiologist. Also delineated as organs at risk (OARs) were the eyes, SVZ, cochlea, pituitary gland, parotids, optic chiasm, brainstem, and whole brain.

To test the effect of applying different treatment margins, the CTVs were expanded around the preoperative tumor bed with isotropic margins of 0.5, 1.0, and 1.5 cm while constraining the lateral, caudal, and anterior extensions of the CTV volumes to be within the PF. Cranially, the CTVs were limited to extending at most 0.5 cm outside of the PF; no limit was applied in the posterior direction. The PTVs for each patient (henceforth referred to as PTV A, PTV B, and PTV C) were expanded from the corresponding CTV volumes with a 0.5-cm isotropic margin. A PTV was also created with a 0.5-cm margin from the PF volume (PTV D) to allow comparison with the

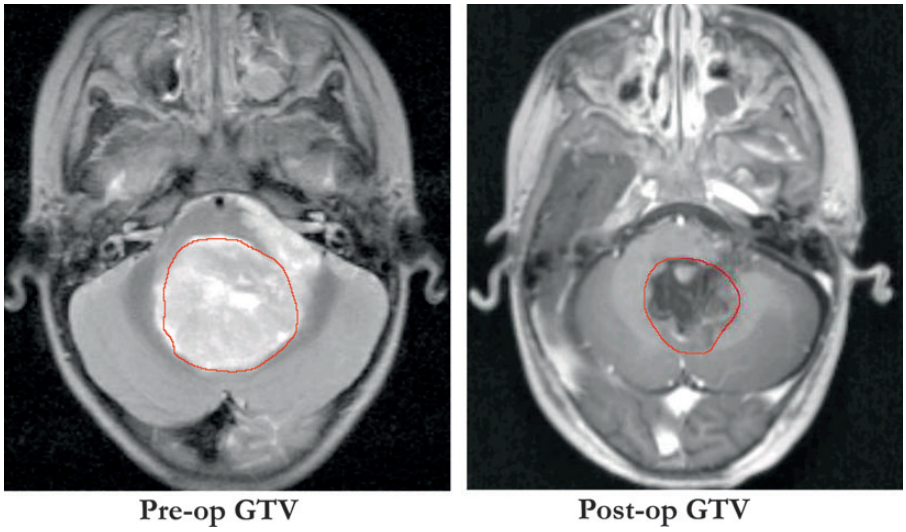

Fig. 1. Different definitions of GTV in MB showing the GTV as the preoperative tumor bed (left panel) and as the postoperative tumor, including operation cavity (right panel), as used in this analysis.

conventional boost treatment. Figure 2 shows an example of the CTV and PTV expansion for one of the patients.

For each patient and for each of the 4 PTVs, individual treatment plans for the high-dose boost were generated with 3D CRT, IMRT, and PT (Eclipse v10, Varian Medical Systems). For the 3D CRT technique, 2 to 4 treatment fields were used, angled from the lateroposterior direction (2 opposed and 2 oblique) with the aim of covering the PTV to the best possible extent. Five fields angled from the posterior direction were used for the inverse-planned IMRT technique, where the main objective was to spare the hippocampus while still achieving good PTV coverage and clinically acceptable doses to the remaining OARs. The same was done for the spot-scanned PT technique but with only a single treatment field from the posterior direction. The different radiotherapy techniques are illustrated for one of the patients in Fig. 3.

The tradeoff between sparing the hippocampus and covering the PTV is controlled through a set of dose-volume objectives assigned in the treatment optimization. We started each treatment optimization at a given set of dose-volume objectives (Supplementary material). The objectives for the OARs were set at a level where the optimizer would be pressed to fulfill them for the larger target volumes (PTV C and PTV D); and if an objective was met, it was lowered to further reduce the dose to that structure. The aim of this treatment optimization strategy was to minimize user dependence and thus increase the reproducibility of our results.

Analyzing Dosimetric Data and the Dependence on Target Size and Position

The calculated doses and delineated structures for each patient and treatment plan were exported as DICOM (Digital Imaging and Communications in Medicine) files and analyzed using CERR software (Computational Environment for Radiotherapy Research)[23] to create corresponding dose-volume histograms. Extraction of doses to target and OARs, as well as the corresponding volumes, was carried out based on the dose-volume histograms using MATLAB software (MathWorks).

The total prescribed dose was 54 Gy to the boost target volume, planned as 23.4 Gy from the CSI and 30.6 Gy from the boost treatment. In a previous analysis,[17] we derived dosimetric relationships between hippocampal dose and the percentage of the whole brain that received at least 95% of the prescribed dose. The hippocampal dose contribution stemming from whole-brain irradiation was taken as the dose that corresponded to 95% of the whole brain receiving at least 95% of the prescribed dose for each of 3D CRT, IMRT, and PT and was added to the hippocampal dose from the boost treatment. We included uncertainty in the CSI hippocampal dose contribution by including the range of estimated doses among the patients in the previous analysis.

We tested for a correlation between the volume of the boost PTV and the absorbed dose to the hippocampus. We also tested whether a simple metric describing the distance or overlap between PTV and the hippocampus could be used as a surrogate to predict the hippocampal dose from the boost treatment.

Estimating the Neurocognitive Impairment Risk for the Different Treatment Techniques and Margins

We used recently published dose-response models for estimating the long-term risk of impaired task efficiency, organization, and memory to estimate the risk of neurocognitive impairment.[17] These logistic dose-response models were derived based on cognitive outcome data from long-term survivors of childhood CNS malignancies, stratified into a group of only patients with MB/primitive neuroectodermal tumor.[4] The length of follow-up of these survivors suggests that the risk of neurocognitive decline can persist for up to 30 years after treatment. The models stem from the relationship between temporal lobe dose and the corresponding type of cognitive impairment. In the current analysis, we make the ansatz that the

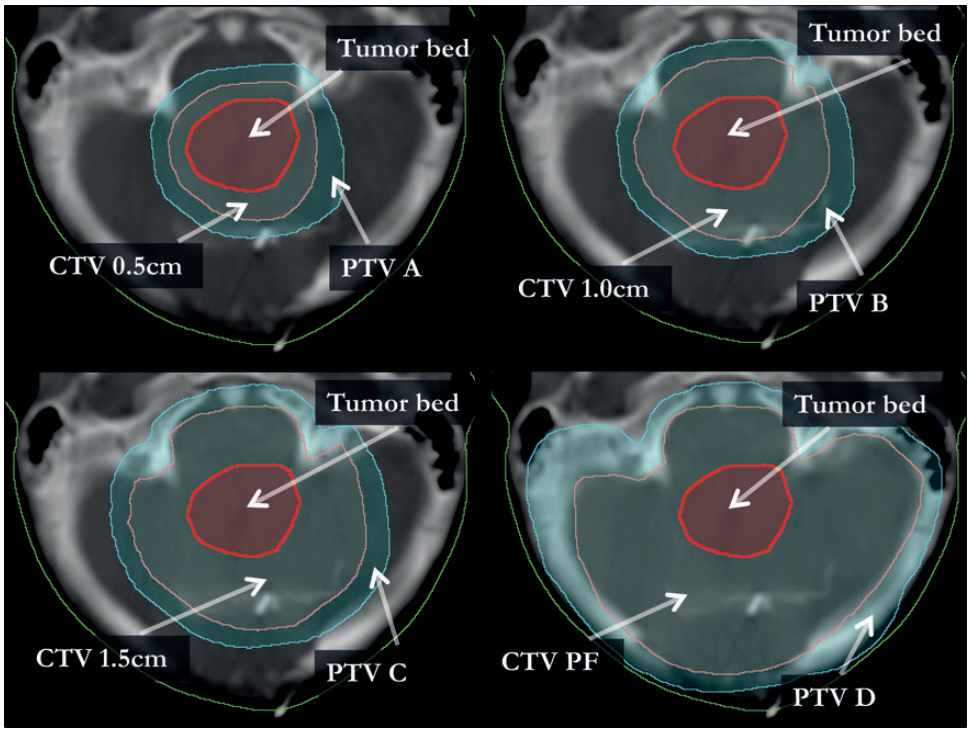

Fig. 2. The expansion of CTV and PTV is shown in relation to the tumor bed on a transversal CT image. This illustrates the difference in the resulting target volume for one patient based on which CTV margin is applied, with a CTV to PTV margin of 0.5 cm in all scenarios.

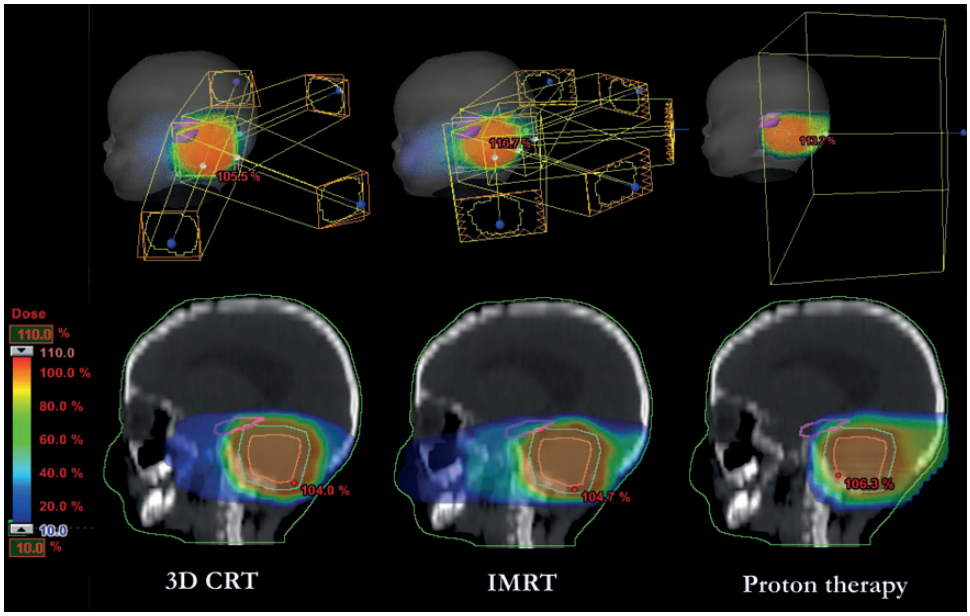

Fig. 3. An example of the field setup for the different radiotherapy techniques and the resulting dose distributions in color-wash for one patient. The target, which in this example is the PTV B, is shown in cyan and the hippocampus is the magenta-colored structure.

dose-risk estimates for the hippocampus alone are the same as the dose-risk estimates for the entire temporal lobe. This corresponds to assuming that the hippocampus is the key structure for radiation-induced neurocognitive decline following temporal lobe irradiation. The dose-response models are given by the following relation:

$$p_D = \frac{OR_{10}^{D/10\,\mathrm{Gy}}}{(1/p_0 - 1) + OR_{10}^{D/10\,\mathrm{Gy}}}$$

where D is the absorbed dose, in grays; OR_{10} is the odds ratio (OR) for the given impairment at 10 Gy; p_0 is the baseline risk of impairment at zero dose; and p_D is the risk of impairment at dose D. The baseline risks were taken from patients in the CNS survivor cohort who did not receive any temporal lobe irradiation.[4] The given OR_{10} values with 95% confidence intervals (CIs) are 2.95 (1.66–5.22), 2.21 (1.04–4.70), and 1.45 (0.91–2.30) for impaired task efficiency, organization, and memory, respectively. The corresponding baseline risks (p_0) are 24.0%, 12.3%, and 24.6%. The mean hippocampal dose from each of the different treatment plans was entered along with the different ORs into the equation to estimate the risk of the respective neurocognitive impairments.

Statistical Analysis

For the estimated risks of cognitive impairment, the largest uncertainty stems from the ORs used in the dose-response models, which are given with 95% CIs. For each of the neurocognitive endpoints, a Monte Carlo sampling technique was applied by randomly drawing 10 000 samples from log-normal distributions matching the mean and 95% CI of the OR_{10} dose-response parameters. We then derived the mean and 95% CI of the estimated risk of impairment in each of the samples. Finally the 95% CI was extracted as the 2.5–97.5 percentile of the 10 000 risk estimate values, averaged over the patient group.

To test whether the estimated risk of impairment was significantly different between treatment techniques, the difference in risk between 2 treatment techniques was extracted for each of the 10 000 Monte Carlo samples. The mean and 95% CI of risk difference for the whole patient group was then calculated by inverse variance weighting of the difference estimates for each patient. To account for potential underestimation of the variance due to the relatively small number of patients, this was done using a bootstrapping procedure. Here, 100 000 samples of the 17 patients were drawn with replacement. A point estimate and 95% CI of the mean risk difference was derived for each sample as explained above. A normal distribution was matched to each of these point estimates and CIs. One sample was then randomly drawn from each of the 100 000 distributions, giving the final risk difference between treatment techniques with 95% CI as the 2.5–97.5 percentile of these randomly drawn samples.

The association between PTV size and hippocampal dose was estimated using Spearman's rank correlation coefficient (Spearman's ρ). Whether these correlations were statistically significant was tested by bootstrapping over the data for the 17 patients. For each correlation analysis, 1 000 000 bootstrap samples were drawn with replacement and the corresponding Spearman's ρ calculated for each sample. The 95% CIs of the correlation coefficients were taken as the 2.5–97.5 percentile of the randomly sampled Spearman's ρ coefficients. The correlations were considered statistically significant if the 95% CI of Spearman's ρ did not cross zero. Corresponding one-sided P values were estimated as the proportion of sampled correlation coefficients that did cross zero in the direction (negative or positive) opposite of the point estimate.

Results

The resulting tumor bed and target volumes for the different treatment margins are presented in Table 1.

Figure 4 shows the spatial distribution of delineated tumor bed volumes and hippocampi between patients.

The resulting hippocampal doses for each treatment technique and target volume are shown in Table 2, with and without the dose contribution from the whole-brain part of treatment. The mean doses from the boost treatment to all other OARs included in this study are also given in Table 2. As expected, a larger boost target volume results in higher dose to the hippocampus. Both of the

Table 1. Median target volumes (range) for the 17 patients

Target Structure	Tumor Bed, GTV	CTV 0.5 cm	CTV 1.0 cm	CTV 1.5 cm	CTV PF	PTV A	PTV B	PTV C	PTV D
Volume, cm^3	17.2 (2.9–60.9)	42.0 (12.0–107.4)	71.3 (30.5–131.8)	107.1 (57.3–185.1)	161.0 (115.2–267.0)	81.9 (30.0–187.3)	127.8 (62.1–224.7)	177.8 (104.6–261.3)	276.2 (213.2–420.2)

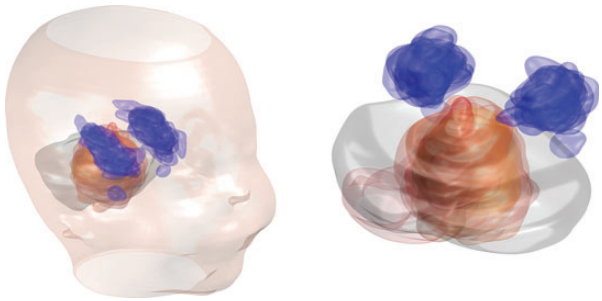

Fig. 4. The spatial distribution of delineated primary tumor beds in relation to the hippocampi for the patients in our cohort. The tumor beds are shown in red and the hippocampi in blue with the semitransparent structures for all patients overlaid on each other. The locations of these structures are overlaid on a single PF contour representative of most PF volumes in our patient group. For graphical clarity, the tumor beds for 2 patients with very irregular size and outlying position of their operation cavities were excluded from this illustration (these were, however, included in all quantitative analyses).

hippocampal sparing techniques result in a substantial reduction in mean dose to the hippocampus. For the remaining OARs, PT resulted in lower doses across the board compared with the photon techniques ($P < .003$ for all OARs and margins in the Wilcoxon signed rank test). The IMRT plans were superior compared with 3D CRT for sparing the cochlea ($P < .001$), parotids ($P < .002$), and whole brain (although not statistically significant, $P > .1$ for all margins) while resulting in higher doses to the optic chiasm ($P < .05$ for all target margins except the PF), pituitary gland ($P < .045$), and the eyes ($P < .003$). The SVZ received virtually no dose from the boost regardless of treatment technique and margin.

Figure 5 shows the distribution of hippocampal doses between patients for the different boost treatment scenarios, illustrating an approximately linear increase in dose with treatment margin.

There were statistically significant correlations between the size of the PTV, in cubic centimeters, and the mean hippocampal dose, with a Spearman's ρ of 0.61 (95% CI: 0.33–0.85) for 3D CRT, 0.62 (95% CI: 0.34–0.84) for IMRT, and 0.59 (95% CI: 0.31–0.83) for PT, all with one-sided P values $<.0001$. The size of the PTV is, however, not an optimal measure to predict the hippocampal dose, since it does not consider how the PTV is positioned in relation to the hippocampus. We found that a well-suited simple metric for predicting the hippocampal dose in our patient group was the distance from the closest point of the PTV to the hippocampal center of mass (taken as the average distance to the center of mass of the left and right part of the hippocampus). This distance was calculated by a MATLAB script developed in-house, and the closest point was found by calculating the Euclidean distances for all surface points of the PTV to the center of mass and choosing the minimal result for left and right hippocampi. For distances up to 2 cm, we fitted linear models with 95% prediction bounds describing the relation between this distance and the mean hippocampal dose as shown in Fig. 6. This linear relation does not hold for larger distances, since the lowest achievable hippocampal dose, for the respective treatment techniques, appears to be reached. This seems to occur at a distance of ~2 cm for PT, 2.5 cm for IMRT, and ~3–4 cm for 3D CRT, suggesting that if the distance between the closest PTV point and the hippocampus center is larger than this, there is no additional benefit from hippocampal sparing.

The estimated risks of neurocognitive impairment, based on the mean hippocampal dose from the boost and whole-brain treatment, are shown in Fig. 7. The estimated risks are considerably lower for PT compared with the photon techniques. Although the 95% CIs are quite wide, the estimated risks with PT were significantly lower for all treatment margins in a paired statistical comparison (Table 3). There was a significant difference between IMRT and 3D CRT in estimated impaired organization and task efficiency. There was also a difference between treatment margins, which again appears to linearly increase when moving to larger treatment margins. Thus, there is a potential for reducing the risk of neurocognitive impairment through smaller target margins for the high-dose boost, although the most substantial risk reduction is estimated to come from applying hippocampal sparing.

Discussion

To the best of our knowledge, this is the first study to perform a detailed investigation of the radiation dose to the hippocampus from the combined course of radiotherapy including varying margins for the high-dose boost in MB treatment. The effect on hippocampal dose from varying treatment margins was an approximately linear increase in dose with increasing target margin. This did, however, also depend on the location of the primary tumor bed.

Although the size of the tumor bed target for the high-dose boost varied considerably among the 17 patients in our study, most tumors were located close to the central axis of the posterior cranial fossa. Most noteworthy is that the reduction in hippocampal dose from using smaller treatment volumes is modest compared with applying a hippocampal sparing technique.

Here, we consider the dose contribution from both the whole-brain part of CSI[17] and the high-dose boost. As expected, the relative dose contribution to the hippocampus is mainly from whole-brain irradiation (Table 2), although this also depends on the size of boost margins as well as how much of the high-dose boost is prescribed from the CSI versus the boost treatment. The results presented here can, however, be extrapolated to alternative MB treatment regimens.

Performing hippocampal sparing requires access to high-resolution MRI scans fused with CT images for radiation treatment

Table 2. Mean doses in Gy (range) from the boost treatment of 30.6 Gy (23.4–54 Gy) for each treatment technique and margin

Treatment technique	3D CRT				IMRT				PT			
Target/risk organ	PTV A	PTV B	PTV C	PTV D	PTV A	PTV B	PTV C	PTV D	PTV A	PTV B	PTV C	PTV D
Hippocampus, boost dose	14.3 (0.4–25.5)	18.0 (0.7–28.1)	20.6 (1.1–28.9)	25.9 (17.0–29.4)	6.9 (2.2–13.8)	9.5 (2.4–15.8)	11.8 (2.7–20.9)	14.4 (9.9–22.3)	3.3 (0.0–8.6)	6.1 (0.0–12.8)	8.7 (0.0–17.9)	11.4 (7.9–17.6)
Hippocampus, total dose*	36.6 (22.7–47.7)	40.2 (23.0–50.3)	42.8 (23.3–51.1)	48.2 (39.3–51.7)	24.4 (18.5–32.2)	27.0 (18.7–34.3)	29.3 (18.9–39.3)	31.9 (26.2–40.8)	10.5 (2.7–17.8)	13.3 (2.7–22.0)	15.9 (2.7–27.1)	18.6 (10.7–26.7)
Cochlea	17.9 (0.7–28.6)	22.0 (1.1–30.0)	24.9 (2.0–30.0)	30.2 (29.2–31.3)	11.6 (4.0–18.4)	14.8 (5.6–20.7)	17.8 (8.3–23.7)	24.2 (21.0–27.6)	4.9 (0.0–15.5)	10.0 (0.0–19.8)	14.3 (0.0–22.2)	19.3 (16.3–22.8)
Pituitary gland	2.9 (0.3–6.6)	5.9 (0.5–15.3)	10.4 (0.7–24.7)	17.9 (1.0–29.0)	8.4 (1.1–18.3)	10.8 (1.4–25.4)	12.5 (1.7–27.0)	15.1 (1.0–29.4)	0.6 (0.0–9.2)	1.0 (0.0–10.8)	3.3 (0.0–20.1)	10.5 (0.3–28.0)
Eyes	0.6 (0.0–5.4)	0.7 (0.1–5.9)	0.9 (0.1–7.0)	1.3 (0.4–7.3)	1.9 (0.5–3.8)	2.4 (0.7–4.6)	2.9 (0.8–5.5)	3.6 (1.8–5.4)	0.0 (0.0–0.0)	0.0 (0.0–0.0)	0.0 (0.0–0.1)	0.1 (0.0–1.7)
Parotids	6.1 (0.4–15.3)	8.2 (1.0–17.3)	10.1 (2.0–18.8)	11.5 (1.1–19.0)	3.3 (1.0–7.1)	4.3 (1.5–8.1)	5.2 (2.1–8.7)	6.3 (2.2–9.8)	0.0 (0.0–0.3)	0.3 (0.0–1.6)	1.0 (0.0–3.8)	3.7 (0.0–9.2)
Optic chiasm	2.5 (0.2–9.1)	4.2 (0.3–12.7)	7.4 (0.4–20.1)	12.8 (4.3–22.7)	7.9 (1.5–13.9)	9.7 (1.8–16.7)	11.2 (1.9–18.1)	14.2 (5.4–20.3)	0.0 (0.0–0.2)	0.4 (0.0–2.5)	2.0 (0.0–9.9)	6.5 (0.2–19.0)
Whole brain	6.1 (1.8–13.1)	7.1 (2.8–13.5)	8.0 (3.8–13.9)	8.7 (5.7–12.2)	5.9 (2.7–13.0)	6.9 (3.6–13.3)	7.8 (4.6–13.8)	8.6 (5.8–12.8)	3.8 (1.2–7.9)	4.8 (2.0–8.5)	5.6 (2.8–9.2)	6.8 (5.0–8.2)
SVZ	0.4 (0.1–1.1)	0.5 (0.1–1.2)	0.7 (0.2–1.4)	0.9 (0.5–2.1)	1.1 (0.3–3.3)	1.3 (0.4–4.8)	1.5 (0.5–6.0)	1.8 (0.6–7.5)	0.0 (0.0–0.0)	0.0 (0.0–0.0)	0.0 (0.0–0.0)	0.0 (0.0–0.0)

*Hippocampal dose from 23.4 Gy whole-brain irradiation and boost treatment of 30.6 Gy.

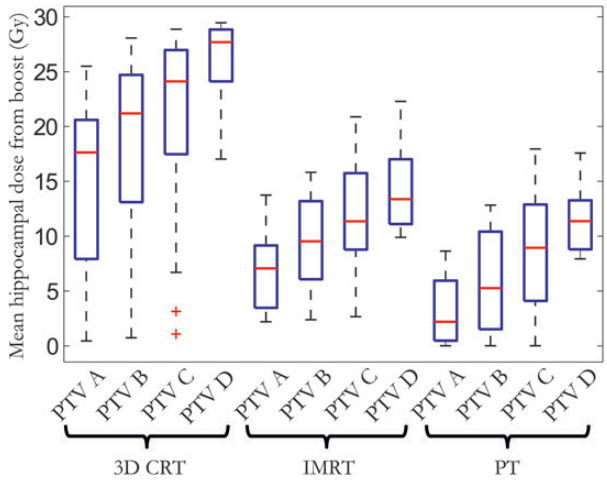

Fig. 5. Distribution of mean hippocampal dose among the 17 patients in this study presented in a box-and-whiskers plot for the different treatment techniques and target volumes. The red horizontal bar shows the median, the box edges the 25th and 75th percentiles, and the whiskers the range of mean doses. Outliers are plotted as red plus signs.

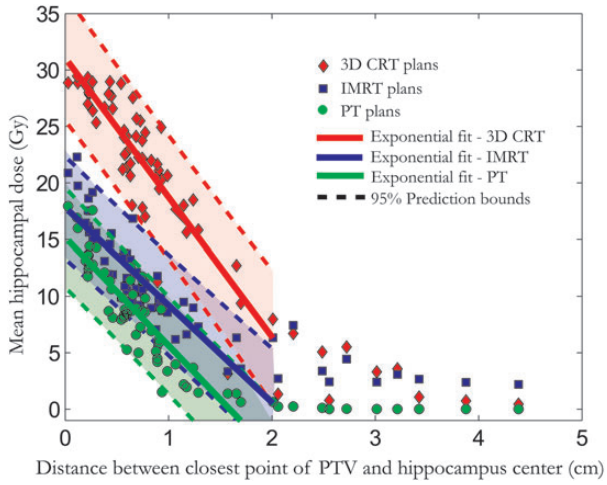

Fig. 6. Mean hippocampal dose from the boost treatment vs the distance between closest point of the PTV and hippocampus center of mass is shown for the 3 different treatment techniques. The 95% prediction bounds give the 95% certainty for estimating the hippocampal dose based on this distance.

planning. Contouring the hippocampus and other intracranial structures requires an experienced neuroradiologist. The Radiation Therapy Oncology Group trial 0933 for hippocampal sparing of patients with brain metastases provides a hippocampal contouring atlas, which may aid in delineation.[24]

We also estimated a considerable clinical benefit of applying a hippocampal sparing approach using modern radiotherapy techniques. The estimated risks of neurocognitive impairment are based on long-term follow-up data from 818 survivors of pediatric CNS malignancies presented by Armstrong et al.[4] These estimates are subject to the statistical uncertainty in the dose-response parameters as well as the uncertainty in data collection through

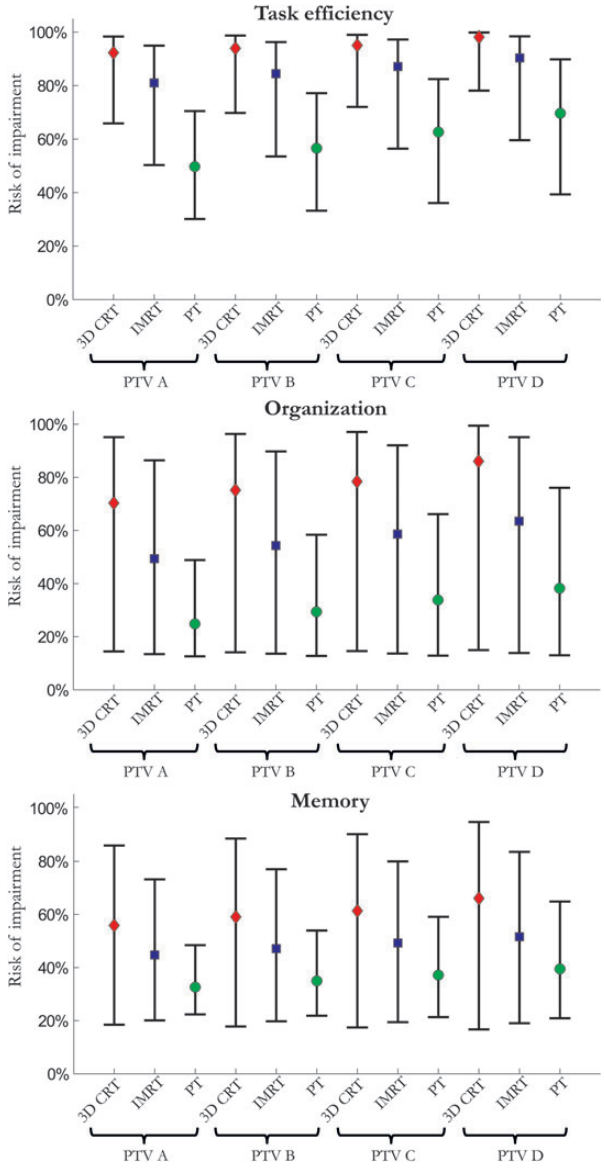

Fig. 7. The estimated risk of impaired task efficiency, organization, and memory is presented for each treatment technique and margin for a craniospinal dose of 23.4 Gy and a high-dose boost up to 54 Gy. The vertical bars show the 95% CIs estimated through 10 000 Monte Carlo samples over the uncertainty in the corresponding dose-response parameters.

neurocognitive testing questionnaires and retrospective dosimetry applied in the Armstrong study. Also, we assume that sparing the hippocampus was equivalent to sparing the whole temporal lobe in the Armstrong study with respect to neurocognitive functioning. This assumption is further strengthened by a recent prospective study by Redmond et al,[10] who showed a significant correlation between decreased motor speed and dexterity on one hand and mean dose to the hippocampus and the temporal lobe on the other. This suggests that mean hippocampal dose is an appropriate metric for estimating neurocognitive impairment, although this should be validated in larger patient material.

Redmond and colleagues found no significant correlation between neurocognitive outcome and dose to the SVZ, consistent with the unclear role of SVZ irradiation in this setting. Hence we did not consider it as a cognitive risk organ in this study. In addition to hippocampal irradiation, the tumor itself as well as surgery and aggressive chemotherapy are likely contributors to cognitive decline. Irradiating the cerebellum to high doses might also add to the risk of cognitive decline, as this could interrupt supratentorial connections between the cerebellum and the frontal part of the brain, as suggested by Armstrong et al.[4] Although this may be attributed in part to the surgical resection, it may be a further argument for applying a conformal tumor bed boost, rather than boosting the whole PF. The cerebellar contribution to cognitive functioning is still poorly understood,[25] making it difficult to assess the importance of such an effect. Irradiating the prefrontal cortex in the whole-brain treatment likely also plays a role in the cognitive decline of MB patients.[26]

Factors such as surgery, hydrocephalus, and chemotherapy also attribute to the risk of neurocognitive decline, as demonstrated by the baseline risk without any temporal lobe irradiation in the applied dose-response models.[17] Incorporating these factors into multivariate dose-response models would allow for better risk estimation and identification of patients who would benefit from hippocampal sparing. Unfortunately, current clinical data do not allow for the quantification of these effects in a multivariate setting.

We showed that it may be possible to predict the mean hippocampal dose based on the distance between the closest point of the PTV and the center of the hippocampus (average between left and right). Measuring this distance for an MB patient before engaging in time-consuming treatment planning can provide estimates of the hippocampal dose and corresponding risk of cognitive impairment depending on the choice of treatment technique. This simple metric could thus help the radiation oncologist evaluate whether the patient should receive the boost treatment

Table 3. Bootstrapped risk differences (95% CIs) between treatment techniques

Risk difference, %	3D CRT – IMRT				IMRT – PT			
Target/risk organ	PTV A	PTV B	PTV C	PTV D	PTV A	PTV B	PTV C	PTV D
Task efficiency, %	11 (4–19)	9 (3–17)	8 (1–15)	8 (1–14)	31 (24–39)	28 (19–37)	25 (15–34)	21 (12–29)
Organization, %	21 (5–36)	21 (4–36)	20 (3–35)	23 (6–39)	25 (14–34)	25 (14–36)	25 (13–37)	25 (12–39)
Memory, %	11 (−1–22)	12 (−1–23)	12 (−1–24)	14 (1–28)	12 (5–19)	12 (4–20)	12 (4–21)	12 (3–22)

Differences are statistically significant at the 5% level if the lower limit of the 95% CI does not cross zero.

with PT, which is not yet widely available, and/or whether the patient would benefit from hippocampal sparing radiotherapy.

The importance of limiting the dose to the hippocampus in pediatric patients receiving cranial irradiation is becoming increasingly evident. Here, we present a detailed analysis of the dose to the hippocampus and corresponding risks of neurocognitive impairment from the high-dose boost in MB treatment. Proton therapy shows most promise for hippocampal sparing due to the very sharp dose gradients achievable through the physical differences in energy deposition compared with photons. Availability of PT is still limited and here we showed that considerable hippocampal sparing is also possible using IMRT, which makes this an attractive alternative option.

When limiting the boost treatment volume to reduce the risk of cognitive decline, one needs to take into account the potential increase in risk of local relapse. There have been several pediatric MB studies using conformal boost treatment instead of previous whole PF irradiation, with excellent PF control rates ranging from 85% to 100%.[6,18–22] Also, recent analyses of recurrence patterns in MB patients did not find sites of relapse to be correlated to treatment deviations or underdosage.[27,28]

In this analysis, we predict a correlation of cognitive outcome with the selection of treatment margins. Specifically, treating with smaller margins from the tumor bed to the PTV compared with whole PF irradiation is estimated to reduce the risk of cognitive decline. However, the decrease in risk of neurocognitive impairment estimated must be balanced against reducing the dose inside parts of the classical target volume. Although the hippocampus corresponds to only ∼1% of the whole-brain volume, limiting the dose here could potentially increase the risk of tumor recurrence. Clearly, hippocampal sparing should therefore be pursued within the setting of a prospective clinical trial in order to validate its effectiveness and safety.

With the increasing availability of PT in Europe and the United States, a prospective trial of hippocampal sparing radiotherapy for MB is attractive. The main challenge in such a trial design will be to demonstrate noninferiority with respect to tumor control, at the same time as demonstrating a benefit in neurocognitive outcome. A detailed pattern of failure analysis in a prospective trial setting may aid by systematically investigating whether failures occur close to the underdosed hippocampal region. There are several other important factors to consider as well, such as treatment robustness and potential risk-group stratification according to histology or the different molecular subgroups of MB.

Supplementary Material

Supplementary material is available online at *Neuro-Oncology* (http://neuro-oncology.oxfordjournals.org/).

Funding

This work was supported by the Danish Child Cancer Foundation (to N.P.B.) and the National Cancer Institute (grant no. 2P30 CA 014520–34 to S.M.B.).

Conflict of interest statement. P.M.R has a research agreement with Varian Medical Systems.

References

1. Fossati P, Ricardi U, Orecchia R. Pediatric medulloblastoma: toxicity of current treatment and potential role of proton therapy. *Cancer Treat Rev*. 2009;35(1):79–96.
2. Lannering B, Rutkowski S, Doz F, et al. Hyperfractionated versus conventional radiotherapy followed by chemotherapy in standard-risk medulloblastoma: results from the randomized multicenter HIT-SIOP PNET 4 trial. *J Clin Oncol*. 2012;30(26):3187–3193.
3. Mulhern RK, Merchant TE, Gajjar A, Reddick WE, Kun LE. Late neurocognitive sequelae in survivors of brain tumours in childhood. *Lancet Oncol*. 2004;5(7):399–408.
4. Armstrong GT, Jain N, Liu W, et al. Region-specific radiotherapy and neuropsychological outcomes in adult survivors of childhood CNS malignancies. *Neuro Oncol*. 2010;12(11):1173–1186.
5. Brown PD, Buckner JC, O'Fallon JR, et al. Effects of radiotherapy on cognitive function in patients with low-grade glioma measured by the Folstein mini-mental state examination. *J Clin Oncol*. 2003; 21(13):2519–2524.
6. Carrie C, Grill J, Figarella-Branger D, et al. Online quality control, hyperfractionated radiotherapy alone and reduced boost volume for standard risk medulloblastoma: long-term results of MSFOP 98. *J Clin Oncol*. 2009;27(11):1879–1883.
7. Grill J, Renaux VK, Bulteau C, et al. Long-term intellectual outcome in children with posterior fossa tumors according to radiation doses and volumes. *Int J Radiat Oncol Biol Phys*. 1999;45(1): 137–145.
8. Jalali R, Mallick I, Dutta D, et al. Factors influencing neurocognitive outcomes in young patients with benign and low-grade brain tumors treated with stereotactic conformal radiotherapy. *Int J Radiat Oncol Biol Phys*. 2010;77(4):974–979.
9. Mulhern RK, Kepner JL, Thomas PR, Armstrong FD, Friedman HS, Kun LE. Neuropsychologic functioning of survivors of childhood medulloblastoma randomized to receive conventional or reduced-dose craniospinal irradiation: a Pediatric Oncology Group study. *J Clin Oncol*. 1998;16(5):1723–1728.
10. Redmond KJ, Mahone EM, Terezakis S, et al. Association between radiation dose to neuronal progenitor cell niches and temporal lobes and performance on neuropsychological testing in children: a prospective study. *Neuro Oncol*. 2013;15(3):360–369.
11. Eriksson PS, Perfilieva E, Bjork-Eriksson T, et al. Neurogenesis in the adult human hippocampus. *Nat Med*. 1998;4(11):1313–1317.
12. Palmer TD, Takahashi J, Gage FH. The adult rat hippocampus contains primordial neural stem cells. *Mol Cell Neurosci*. 1997;8(6): 389–404.
13. Acharya MM, Christie LA, Lan ML, et al. Rescue of radiation-induced cognitive impairment through cranial transplantation of human embryonic stem cells. *Proc Natl Acad Sci U S A*. 2009;106(45): 19150–19155.
14. Shors TJ, Miesegaes G, Beylin A, Zhao M, Rydel T, Gould E. Neurogenesis in the adult is involved in the formation of trace memories. *Nature*. 2001;410(6826):372–376.
15. Raber J, Rola R, LeFevour A, et al. Radiation-induced cognitive impairments are associated with changes in indicators of hippocampal neurogenesis. *Radiat Res*. 2004;162(1):39–47.
16. Rola R, Raber J, Rizk A, et al. Radiation-induced impairment of hippocampal neurogenesis is associated with cognitive deficits in young mice. *Exp Neurol*. 2004;188(2):316–330.

17. Blomstrand M, Brodin NP, Munck Af RP, et al. Estimated clinical benefit of protecting neurogenesis in the developing brain during radiation therapy for pediatric medulloblastoma. *Neuro Oncol*. 2012;14(7): 882–889.
18. Douglas JG, Barker JL, Ellenbogen RG, Geyer JR. Concurrent chemotherapy and reduced-dose cranial spinal irradiation followed by conformal posterior fossa tumor bed boost for average-risk medulloblastoma: efficacy and patterns of failure. *Int J Radiat Oncol Biol Phys*. 2004;58(4):1161–1164.
19. Gupta T, Jalali R, Goswami S, et al. Early clinical outcomes demonstrate preserved cognitive function in children with average-risk medulloblastoma when treated with hyperfractionated radiation therapy. *Int J Radiat Oncol Biol Phys*. 2012;83(5):1534–1540.
20. Paulino AC, Mazloom A, Teh BS, et al. Local control after craniospinal irradiation, intensity-modulated radiotherapy boost, and chemotherapy in childhood medulloblastoma. *Cancer*. 2011;117(3): 635–641.
21. Polkinghorn WR, Dunkel IJ, Souweidane MM, et al. Disease control and ototoxicity using intensity-modulated radiation therapy tumor-bed boost for medulloblastoma. *Int J Radiat Oncol Biol Phys*. 2011;81(3): e15–e20.
22. Wolden SL, Dunkel IJ, Souweidane MM, et al. Patterns of failure using a conformal radiation therapy tumor bed boost for medulloblastoma. *J Clin Oncol*. 2003;21(16):3079–3083.
23. Deasy JO, Blanco AI, Clark VH. CERR: a computational environment for radiotherapy research. *Med Phys*. 2003;30(5):979–985.
24. Gondi V, Tomé WA, Rowley HA, Metha MP. Hippocampal contouring: a contouring atlas for RTOG 0933. http://www.rtog.org/CoreLab/ContouringAtlases/HippocampalSparing.aspx. Accessed May 16, 2013.
25. Baillieux H, De Smet HJ, Paquier PF, De Deyn PP, Marien P. Cerebellar neurocognition: insights into the bottom of the brain. *Clin Neurol Neurosurg*. 2008;110(8):763–773.
26. Euston DR, Gruber AJ, McNaughton BL. The role of medial prefrontal cortex in memory and decision making. *Neuron*. 2012;76(6): 1057–1070.
27. Perreault S, Lober RM, Carret AS, et al. Relapse patterns in pediatric embryonal central nervous system tumors. *J Neurooncol*. 2013; 115(2):209–215.
28. Warmuth-Metz M, Blashofer S, von Bueren AO, et al. Recurrence in childhood medulloblastoma. *J Neurooncol*. 2011;103(3):705–711.